Electron Holographic Observations of the Electrostatic Field Associated with Thin Reverse-Biased p-n Junctions

Stefano Frabboni, Giorgio Matteucci, and Giulio Pozzi

Center for Electron Microscopy and Centro Italiano di Struttura della Materia/Gruppo Nazionale di Struttura della Materia–Consiglio Nazionale delle Ricerche, Department of Physics, University of Bologna, 40126 Bologna, Italy

and

Massimo Vanzi

Reliability and Quality Department, Telettra S.p.A., 20059 Vimercate (Mi), Italy

(Received 5 August 1985)

A new method has been devised for investigation by transmission electron microscopy of the electrostatic microfield associated with reverse biased p-n junctions. By means of electron holography and optical interferometry it is possible to obtain on the reconstructed images two-dimensional representations of the projected potential distribution inside and outside the specimen.

PACS numbers: 73.40.Lq, 42.40.My, 61.16.Di

The introduction of conventional transmission electron microscopes equipped with high-brightness field-emission guns (FEG) has recently stimulated a revival of interest in interference electron microscopy, especially because of the prospects offered by its application to electron holography.[1] In particular, off-axis holographic methods have been successfully applied to the investigation of magnetic microfields in thin films,[2,3] which play an increasingly important role in the development of high-density recording devices.[4] The electron wave can be affected also by electrostatic microfields, such as those associated with reverse-biased p-n junctions contained in specimens which are made transparent to the electrons.

The experience gained in the study of ferromagnetic specimens can therefore be transferred to this research field, whose technological implications are of the utmost importance in view of the very large-scale integration trend toward submicrometer structures. For several years our group has been interested in the investigation of reverse-biased p-n junctions by means of standard Lorentz microscopy[5] and of electron-interferometry methods.[6] Both these techniques essentially provide limited, one-dimensional information across the p-n junction, whereas electron holography is so far the only way to recover the two-dimensional phase distribution of the wave leaving the object.

In this paper we present and discuss the first experimental results obtained by applying electron-holography techniques to the observation of reverse biased p-n junctions.

The procedure to obtain a specimen suitable for transmission electron microscopy from an n-type silicon wafer is shown in Fig. 1. The surface layer of the sample was preamorphized by the implanting of Si^+ ions in order to minimize channeling phenomena. Boron ions with a dose of 1×10^{15} cm^{-2} were successively implanted at 10 keV.[7] The wafer was then annealed at 900 °C for 30 min in a nitrogen atmosphere. The implantation was carried out through a SiO_2 mask consisting of parallel slits 10 μm wide and of 10 μm spacing in order to produce a set of parallel diodes. The resulting p-n junctions have a depth of $x=0.3$ μm, depletion-layer width $W=1.4$ μm, and a built-in potential of $V=0.76$ V.

In order to bias the junctions, one end of the structure made up with parallel slits was electrically shorted by vacuum deposition of a TiAg layer; this continuous layer connects the p regions together and is isolated from the n regions by the SiO_2 layer used for ion implantation. Far from the TiAg layer, the SiO_2 mask was removed by photolithography. A rectangular, flat region was obtained, which consists of a set of p-n junctions. The junctions can be biased with an external emf source applied between the TiAg layer and the back of the wafer. The implanted wafer was subsequently chemically thinned, from the side of the backing material, in correspondence to the region where

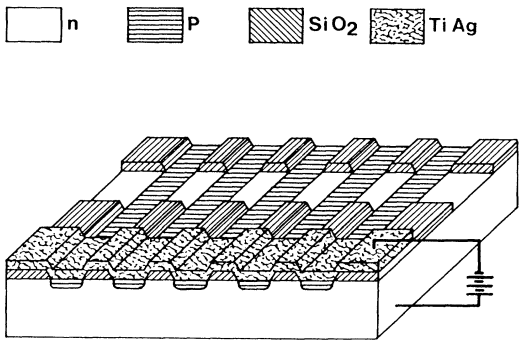

FIG. 1. Schematic drawing of the ion-implanted diodes; n = n-type Si, p = p-type Si.

the SiO_2 mask was removed. By protracting the thinning up to the formation of a hole, it was possible to obtain around it a thin area containing several parallel junctions side by side. Since the lower portion of the junctions has been removed by the thinning process, the remaining part of them is perpendicular to the wafer surface.

In order to carry out the observations in the electron microscope the thinned specimen was mounted on a special specimen holder equipped with electrical contacts for biasing the junctions. When a reverse bias is applied to the array, an enhancement of the electrostatic field of the junctions is produced both inside and outside the specimen.[5,8-10] The inner field lines of the junctions are parallel to the upper-specimen surface and perpendicular to the beam.

Figure 2 is intended to show schematically the trend of the equipotential surfaces around the specimen by means of their intersection with (i) the plane inside the specimen parallel to the direction z of the electron beam, and perpendicular to the junction boundary, and (ii) the xy plane at the edge of the hole H. The equipotential surfaces spread out from the upper and lower surfaces of the specimen where the junctions are localized and extend as far as the edge of the hole where they rotate.

The effect of a specimen containing an electrostatic potential distribution $V(x,y,z)$ on the electron beam can be described by means of a transmission function (object wave function)[1]

$$\psi(x_0,y_0)=\exp[i\phi(x_0,y_0)]. \quad (1)$$

The phase shift $\phi(x_0,y_0)$ is given in the phase-object approximation by

$$\phi(x_0,y_0)=(\pi/\lambda E)\int V(x_0,y_0,z)\,dz, \quad (2)$$

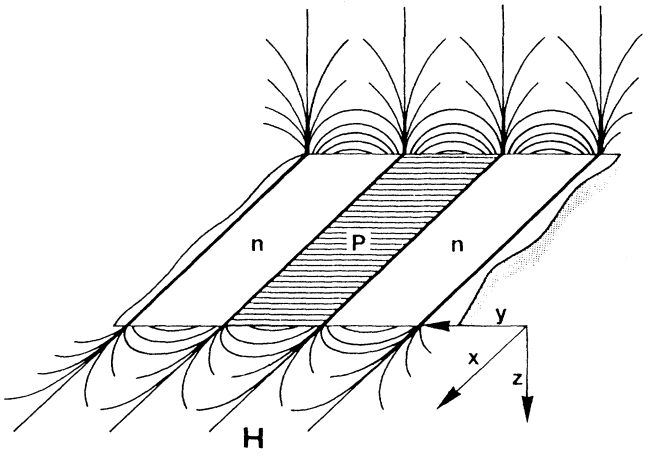

FIG. 2. Sketch of the intersections of the equipotential surfaces associated with the external field of p-n junctions with planes parallel and perpendicular to the optic axis z.

where x_0 and y_0 are the coordinates of a point in the object plane at $z=z_0$ along the optical axis z, λ is the de Broglie wavelength, and E is the accelerating voltage (in the nonrelativistic approximation). The integral is calculated along an electron path parallel to the optical axis z, both inside and outside the specimen.[1] Expression (2) shows that the phase shift encodes the two-dimensional information corresponding to the potential distribution projected onto the xy plane (Fig. 2).

In the case of the electrostatic field associated with the p-n junction in a specimen of constant thickness t, the phase shift can be written as the sum of two terms.[8-10] The first one is related to the internal potential $V_{\rm INT}(x_0,y_0)$ and is of the form

$$\phi_{\rm INT}(x_0,y_0)=(\pi/\lambda E)\,V_{\rm INT}(x_0,y_0)\,t, \quad (3)$$

i.e., it is identical to the contribution given only by the inner potential, which can be included in V. The second term is related to the external field extending around the specimen and can be written in the more general form as a Poisson-type two-dimensional integral of the potential distribution at the specimen surfaces.[10]

Theoretical interpretations of the out-of-focus images show that the external-field contribution is the dominant factor for experiments at standard accelerating voltages (100 kV) and when the specimen thickness t is much smaller than the depletion layer width W.[9] This situation is different from the magnetic case, where it can be shown that the phase shift is expressed in terms of the magnetic vector potential, and the leakage fields can be neglected in most cases.[2,4,11]

The experimental observations were carried out on a Philips EM 400T electron microscope equipped with a FEG. Figure 3 shows an out-of-focus electron image of the specimen area where a p-n junction is present. The reverse bias was 4 V, the defocus distance 1.6 mm, and the electron optical magnification 1700×.

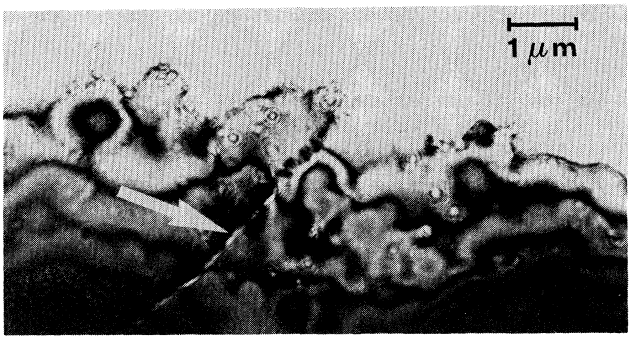

FIG. 3. Out-of-focus image of a region where a p-n junction is present. The arrow marks the contrast line associated with the depletion layer. The junction inner field lies in the plane of the foil.

The arrow points out the bright contrast line which arises in correspondence with the specimen region where the depletion layer is located.

This same region has been investigated by electron holography. A schematic representation of the method used for the formation of off-axis image electron holograms is shown in Fig. 4. A parallel electron beam transmitted through the specimen S is superimposed, by means of the biprism B, on that part of the beam (reference beam R) which travels through the hole H present in the specimen. The resulting hologram, which is formed in the intermediate image plane PO (conjugated to the specimen plane) below the divergent biprism, encodes the phase difference between the two interfering beams. The hologram is further magnified by the projector system onto the final observation plane, and is then recorded on a photographic plate.

With the present state of the art, the recorded electron holograms typically have an interference field of about 200–300 fringes of 50–60-μm spacing, which allows for a resolution of about 3 times the fringe spacing, i.e., 150–200 μm. The distance between the interfering beams is given approximately by the interference field width (the biprism wire diameter is ignored), i.e., about 15 mm in the recording plane.[1] In order to obtain all quantities which correspond to the specimen plane, it is sufficient to divide them by the total magnification. Therefore it turns out that with a high specimen magnification it is possible to achieve high resolution, but correspondingly small distances between interfering beams, and vice versa.

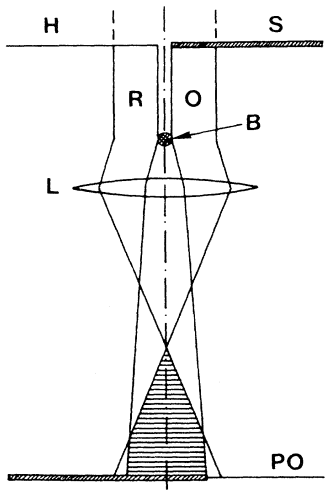

FIG. 4. Hologram formation in the electron microscope. O, ray path corresponding to the object wave through the specimen S; R, reference wave through the hole H; B, electron biprism; L, imaging lens; and PO, observation plane conjugated to the specimen plane.

In the present case it should be noted that the equipotential surfaces associated with the p-n junction extend also into the hole region H (as sketched in Fig. 2) traversed by the reference wave R. Therefore, strictly speaking, R is not an unperturbed wave, but is influenced by the external leakage field distribution. As this field diminishes by an increase in the distance from the hole edge, we tried to minimize this effect by increasing the distance between the interfering beams by working at a low magnification.[6] For this purpose, the objective lens was switched off and the diffraction lens acted as an imaging lens. Under these conditions, the total magnification of the specimen was about 2500, and the distance between the two interfering beams at the specimen level was about 6 μm (approximately 30× larger than when the objective lens was switched on). Such a large value was obtained at the expense of the resolution, which was reduced to 70 nm, but was still sufficient to resolve the depletion layer width (1.4 μm).

The superiority of electron holography, with respect to the standard Lorentz techniques, becomes apparent when we carry out holographic interferometry experiments on an optical bench equipped with a Mach-Zehnder interferometer used as a beam splitter.[1,4] Two laser beams emerging from the Mach-Zehnder equipment illuminate the image electron hologram. The reconstructed wave front of one beam and the conjugate wave front of the other beam are selected through an aperture. From the superposition of these two wave fronts, an interferogram is obtained showing a two-dimensional phase distribution amplified by a factor of 2.

Some of the results obtained by this optical process are shown in Figs. 5(a) and 5(b); they refer to the same area as Fig. 3 for two values of the reverse bias applied to the p-n junction, 4 and 8 V, respectively. The use of a reverse-biased junction is necessary in order to enhance the effect and to check it for genuineness. The specimen edge can be recognized by comparison to Fig. 3 in the lower part of the micrographs. Optical contour lines, representing the projected potential distribution, are superimposed on the image of the specimen, displaying the theoretically expected trend: In the inner specimen regions they are parallel to the junction and to each other, whereas at the edge the lines show a kink and fan out to join the nearest junctions.

It can be noted that the contour lines in Fig. 5(b) display the same trend as those in Fig. 5(a) but their density is doubled as expected.

By comparison of Fig. 5 with Fig. 3 it is evident that the available information is considerably enhanced. Whereas the out-of-focus image displays a contrast line much narrower than the depletion layer width (the contrast arises only from the region having the highest

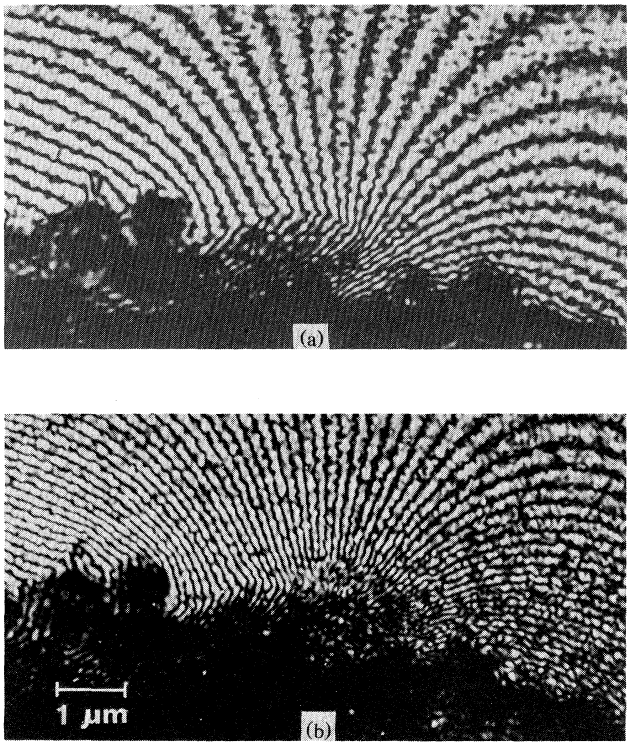

FIG. 5. Optical interferograms of the region surrounding the p-n junction shown in Fig. 3. The reverse bias is (a) 4 V and (b) 8 V. The magnification mark is the same for both images.

object-phase gradient), the contour lines in the optical interferograms cover the whole image field, and their trend and density can be used for a more quantitative evaluation of the electric-field topography and intensity.

In conclusion, the results presented here show that the novel method of electron holography can be successfully applied to the investigation of the electrostatic field distributions of reverse-biased p-n junctions. It requires the use of a FEG, electron and optical interferometers, and a careful specimen preparation technique, which needs further improvements.

In this project the optical method of phase amplification was adopted in order to obtain a system of contour lines which directly and clearly displays the trend of the in-plane projected equipotential surfaces resulting from the superposition of the electric field inside and outside the specimen. It should be pointed out that the holograms can also be processed by many optical techniques, which have no counterpart when the electron microscope is used and which are able to extract the desired information in its useful form.[1]

Particularly interesting is the prospect, outlined in the theoretical work of Ref. 10, of recovering the potential distribution of the internal field by optical or numerical deconvolution of the phase distribution obtained by means of holographic techniques.

We would like to thank E. Gabilli, R. Lotti, P. Negrini, and G. Pizzochero of the Technological Department of the LAMEL Institute of the Italian National Research Council (CNR) for the fabrication of the diodes, and A. Garulli, D. Govoni, and P. Mengucci for technical assistance. We are indebted to Professor U. Valdrè for a critical reading of the manuscript and for providing the specimen holder. Useful discussions with Dr. G. F. Missiroli are also acknowledged. This work has been supported by funds from the Ministero della Pubblica Istruzione, Italia.

[1]G. F. Missiroli, G. Pozzi, and U. Valdrè, J. Phys. E **14**, 649 (1981); K. J. Hanszen, Adv. Electron. Electron Phys. **59**, 1 (1982).

[2]A. Tonomura, T. Matsuda, H. Tanabe, N. Osakabe, J. Endo, A. Fukuhara, K. Shinagawa, and H. Fujiwara, Phys. Rev. B **25**, 6799 (1982); N. Osakabe, K. Yoshida, Y. Horiuchi, T. Matsuda, H. Tanabe, T. Okuwaki, J. Endo, H. Fujiwara, and A. Tonomura, Appl. Phys. Lett. **42**, 746 (1983).

[3]G. Matteucci, G. F. Missiroli, and G. Pozzi, IEEE Trans. Magn. **20**, 1970 (1984).

[4]T. Matsuda, A. Tonomura, R. Suzuki, J. Endo, N. Osakabe, H. Umezaki, H. Tanabe, Y. Sugita, and H. Fujiwara, J. Appl. Phys. **53**, 5444 (1982); N. Osakabe, K. Yoshida, Y. Horiuchi, T. Matsuda, H. Tanabe, T. Okuwaki, J. Endo, H. Fujiwara, and A. Tonomura, Appl. Phys. Lett. **42**, 746 (1983).

[5]P. G. Merli, G. F. Missiroli, and G. Pozzi, Phys. Status Solidi **30**, 699 (1975).

[6]G. Matteucci, G. F. Missiroli, G. Pozzi, P. G. Merli, and I. Vecchi, Thin Solid Films **62**, 5 (1979).

[7]S. Solmi, E. Landi, and P. Negrini, IEEE Electron Device Lett. **5**, 359 (1984).

[8]C. Capiluppi, P. G. Merli, and G. Pozzi, Optik (Stuttgart) **47**, 205 (1977).

[9]P. G. Merli and G. Pozzi, Optik (Stuttgart) **51**, 39 (1978).

[10]M. Vanzi, Optik (Stuttgart) **68**, 319 (1984).

[11]A. Fukuhara, K. Shinagawa, A. Tonomura, and H. Fujiwara, Phys. Rev. B **27** 1839 (1983).

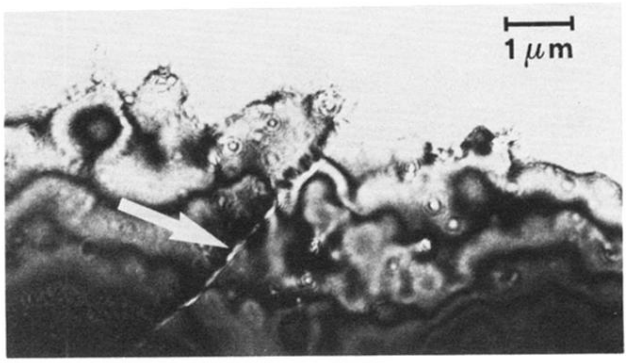

FIG. 3. Out-of-focus image of a region where a p-n junction is present. The arrow marks the contrast line associated with the depletion layer. The junction inner field lies in the plane of the foil.

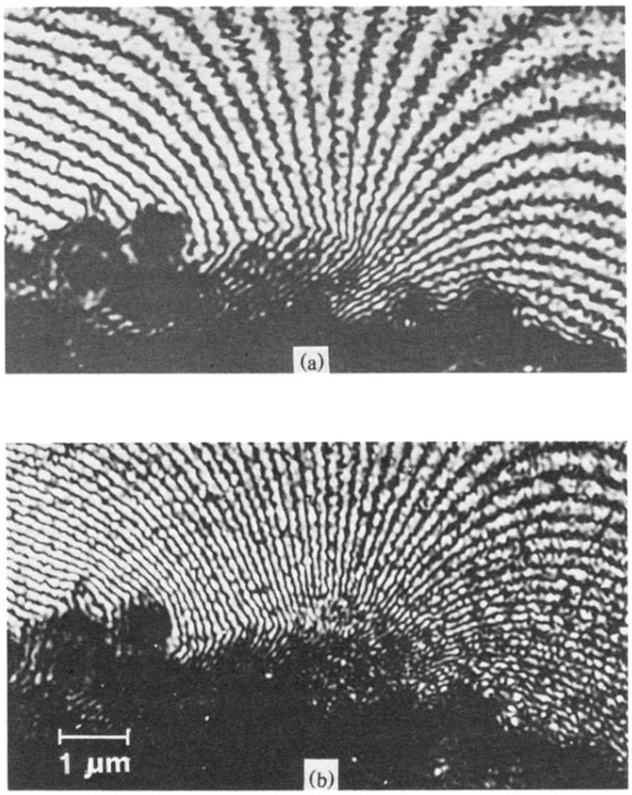

FIG. 5. Optical interferograms of the region surrounding the p-n junction shown in Fig. 3. The reverse bias is (a) 4 V and (b) 8 V. The magnification mark is the same for both images.